Acta Geophysica (2020) 68:783–793
https://doi.org/10.1007/s11600-020-00432-1

RESEARCH ARTICLE - HYDROLOGY

Multiscale comparison of LS factor calculation methods based on different flow direction algorithms in Susa Ancient landscape

Javad Khanifar[1] · Ataallah Khademalrasoul[1]

Received: 27 November 2019 / Accepted: 18 April 2020 / Published online: 28 April 2020

Abstract
Topography (LS factor) is one of the most important controlling factors of soil characteristics and geomorphic processes in the landscape. This study was performed in the Susa Ancient site and aimed to compare the estimation of three different LS factor calculation methods in which the catchment area was calculated based on seven types of flow direction algorithms using DEM with five spatial resolutions. For calculating the LS factor, the catchment area attribute was used to calculate the slope length based on the flow direction. Results showed that the catchment area is an entirely scale-dependent attribute and with decreasing the spatial resolution, the statistical values of catchment area increased. At high spatial resolution, the different flow direction algorithms despite the difference in the flow distribution to the neighboring cells, but the catchment area attributes calculated based on them, are statistically slightly different. By upscaling, the LS factor values calculated in Boehner and Selige and Moore et al. methods increase, whereas in Desmet and Govers method decrease and this change rate indicates that the LS factors calculated by these three methods have the lowest sensitivity to the slope length. At a same scale, the statistics of LS factors calculated based on different flow direction algorithms depicted no considerable different. The single flow direction algorithms of Rh and D8 cause to calculate the lowest mean values of LS factors at all spatial resolutions. The difference between frequency distributions of the LS factors calculated by these three methods increases with decreasing spatial resolution. The statistical analysis of this study confirms that estimating the LS factor scale and calculation method are more important than the type of flow direction algorithm.

Keywords LS factor · DEM · Flow accumulation · Flow routing algorithm · Topography

Introduction

One of the most destructive forms of soil degradation is the soil erosion by water, which is the dominant geomorphic process in many areas of the earth and has adverse effects on the hydrological, geomorphic and biochemical systems in the soil (Zhang et al. 2015; Kinner 2003). In the archeological process, which is based on interpreting the status of objects in the past (the systemic context) through the study of how they exist in the present (the archaeological context), soil erosion is recognized as a serious problem in ancient landscapes because it causes in partial or complete destruction of the archaeological record (Howland et al. 2018). To avoid the negative consequences of soil erosion, especially at archaeological sites, it is necessary to localize and quantify the soil loss in order to select and implement the best management practices (BMPs) for soil conservation. In soil erosion assessment studies have used various empirical-statistical models, one of which being widely used in estimating soil loss is revised universal soil loss equation (RUSLE) (Renard et al. 1991). This model takes into account climatic factors (R), soil erodibility (K), land use (CP) and topography (LS) when assessing soil erosion. The spatial nature of these factors makes it possible to integrate the RUSLE model with geographic information system (GIS) and remote sensing (RS). Topographical attributes such as slope gradient (S) and slope length (L) are considered as the most important land surface properties which control energy fluxes, overland and intrasoil transport of water and sediment, and vegetation cover distribution within a landscape (Zhang et al. 2015, Florinsky 2016). The development of modern techniques such as geomorphometry has made it possible to quantify these attributes in GIS environments. Geomorphometry or

✉ Ataallah Khademalrasoul
a.khademalrasoul@scu.ac.ir; Ataalahsoil@gmail.com

[1] Soil Science Department, Faculty of Agriculture, Shahid Chamran University of Ahvaz, Ahvaz, Iran

terrain analysis is a computer technology-based science in which morphometric and hydrological attributes are calculated by a series of mathematical algorithms from a digital elevation model (DEM) (Pike et al. 2009). An important issue in terrain analysis is the scale, which can have a significant influence on the values distribution of terrain attributes. The term "scale" here refers to spatial resolution, which is a determining factor in representation of landscape details. Moreover, the DEM data with a raster format are equivalent to the pixel size in horizontal directions *X* or *Y*. The effect of spatial resolution on terrain attributes has been studied (Kienzle 2004; Deng et al. 2007). Various guidelines have already been presented for using an optimal scale in terrain analysis, for instance Gessler (1996) finding that a DEM spatial resolution finer than 40 m is required in an erosional landscape (cited by McKenzie and Ryan 1999). However, Zhang and Montgomery (1994) proposed a 10 m spatial resolution for DEM-based modeling of hydrological and geomorphic processes in many landscapes. In the study of Khanifar et al. (2019), the effect of spatial resolution on the geomorphometric modeling of soil properties on a watershed scale was investigated. The results of this study illustrate that the selection of one optimal scale for soil–landscape relationships analysis is a very complex and impossible process and brings this idea conceivable that due to the increase availability to DEMs with high resolution all terrain analysis will be performed in a multiscale framework. Considering the importance of DEM spatial resolution and the topographic factor (LS) in soil erosion modeling, the main objective of this study was to compare the estimation of LS factor calculation methods fitted based on various flow direction algorithms at different scales.

Materials and methods

Location of study area

The study area is the Susa Ancient site with an approximate area of 350 hectares which is located in the center of Khuzestan Province with geographical coordination of 30° 11′ N and 48° 15′ E (Fig. 1). The average temperature of this area is 26 °C, and the average annual precipitation is around 213 mm (based on climate data of 2010–2018). The average altitude of site is about 80 m, and deposits of the fourth periods (Quaternary sediments) are exposed in that. Susa site is a complex consisted of interconnected ancient mounds that serve as important evidence about the process of formation and expansion of the Susa city (ICHHTO 2015).

Digital elevation model

The digital elevation model was constructed from a topographic map with 0.25 m control interval using the ANUDEM interpolation method in ArcGIS environment (ArcMap10.2 software) at 0.25, 0.5, 1, 2 and 3 m spatial

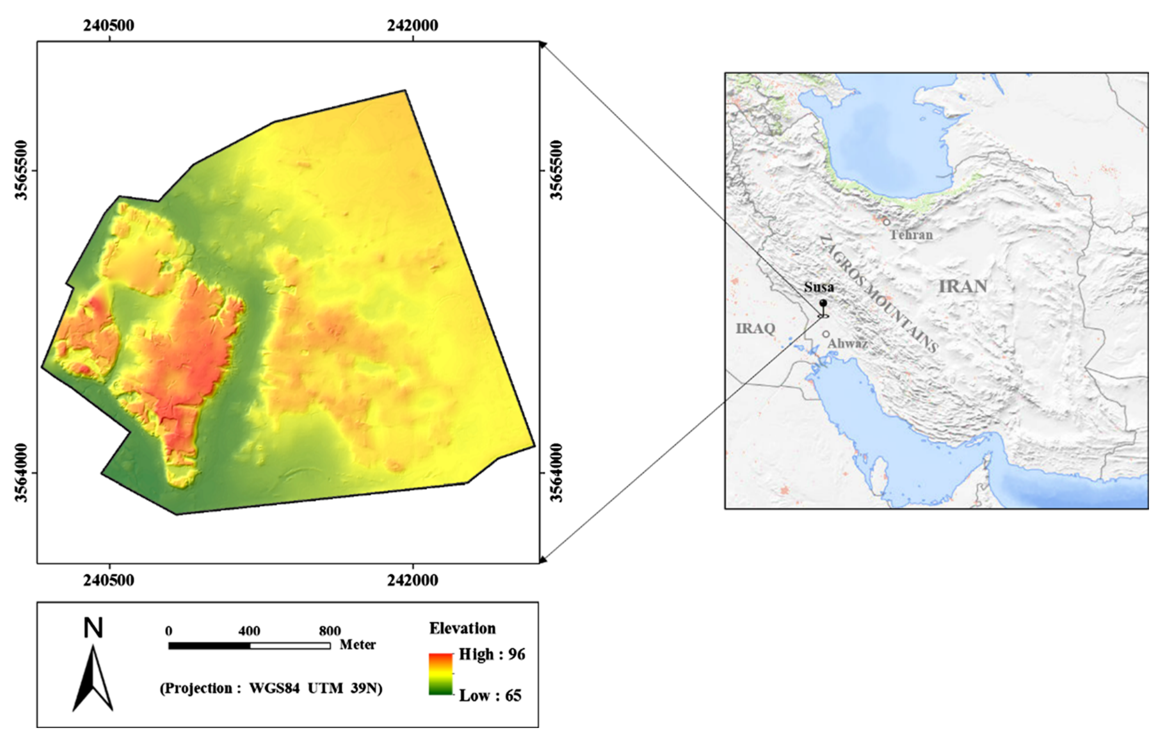

Fig. 1 The location of the study area

resolution (Fig. 2). Prior to the start of geomorphometric analysis, the DEM preprocessing was performed with the aim of eliminating the anomalies in it using the Fill Sink tool in ArcMap10.2 software. The term of anomalies actually refers to a series of unwanted pits that are between elevation data. These unwanted pits lead to discontinuity of drainage network and errors in hydrological modeling, in particular determining the basic attributes of flow direction and flow accumulation.

Topographic factor (LS)

One of the most important factors affecting water erosion and sediment transport is topographic conditions of landscape. In the RUSLE model, the effect of topography on soil erosion is considered by two attributes of slope length (L) and slope steepness (S) in the form of LS factor. Various methods have been presented for calculating this factor, some of them are based on two morphometric attributes of slope gradient (G) and flow accumulation (FA). In this study, topographic factor was calculated based on the methods presented in Table 1. The calculation of slope gradient was performed by Evans (1979) method using the 3×3 plane square-gridded moving neighborhood analysis window in radians unit. Flow accumulation is one of the important hydrological attributes and indicates how much water is collected from the upstream area and contributes to overland flow. It is calculated as the number of upstream cells that flows into each cell according to their flow directions. In the flow accumulation raster, the value of each cell is the number of cells that drain into it. (The cell itself is not included.) The basis of calculation of flow accumulation is the determination of flow direction (Zhu 2016). The flow direction is the most basic geomorphometric attribute related to hydrological modeling, and the fundamental principle in determining this attribute is that the water flows downhill (from a higher to lower place). There are generally two approaches for determination of flow direction: a) single flow direction and b) multiple flow direction (Li et al. 2005). A systematic classification of the algorithms used for the determination of flow direction based on these approaches is done by Zhou and Liu (2002). In this study, the seven types of flow direction algorithms presented in Table 2 are used to determine the flow accumulation and their effect on the LS factor calculation at different scales was investigated. All the processes of calculating the terrain attributes and extracting the values of descriptive statistics (mean, standard deviation and frequency distribution) were performed using SAGA 7.2.0 software. The charts package in Excel 2013

Table 1 Different calculation methods of RUSLE's topographic factor

Equation	Authors
$\left(\frac{\mathrm{CA}^{0.5}}{22.13}\right)^{0.5}.\left(65.14\sin^2\beta_{\mathrm{CA}} + 4.56\sin\beta_{\mathrm{CA}} + 0.065\right)$	Boehner and Selige (2006)
For $\beta_{\mathrm{CA}} > 0.0505$	
$\left(\frac{\mathrm{CA}^{0.5}}{22.13}\right)^{3.\beta_{CA}^{0.6}}.\left(65.14\sin^2\beta_{\mathrm{CA}} + 4.56\sin\beta_{\mathrm{CA}} + 0.065\right)$	
$\frac{(\mathrm{CA}+D^2)^{m+1}-\mathrm{CA}^{m+1}}{D^{m+2}.x^m.(22.13)^m}.S$	Desmet and Govers (1996)
$\left(\frac{\mathrm{SCA}}{22.13}\right)^{0.4}.\left(\frac{\sin\beta}{0.0896}\right)^{1.3}.(1.4)$	Moore et al. (1991)

Catchment area (CA)—discharge contributing upslope area of each grid cell $[\mathrm{m}^2] = \mathrm{FA} \cdot \mathrm{cell\,size}^2$. Specific catchment area (SCA)—catchment area (CA) per unit contour width $[\mathrm{m}^2\,\mathrm{m}^{-1}] = \mathrm{FA} \cdot \mathrm{cell\,size}$. β_{CA}—mean slope of the catchment area. D—raster cell size. X—coefficient that corrects the length of flow way through a raster cell$=\left(\sin\alpha_{i,j} + \cos\alpha_{i,j}\right)$. $\alpha_{i,j}$ = aspect direction of the grid cell (i, j). m—index of slope's length factor that related to the F ratio of the rill to interrill erosion (McCool et al. 1989). S—slope steepness factor calculated by McCool et al. (1989) method. β—slope gradient [radians]. LS factor is dimensionless

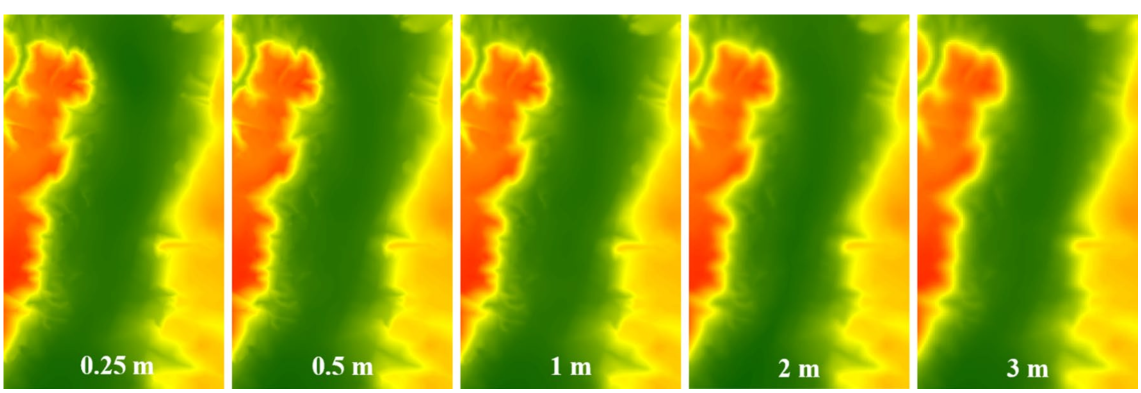

Fig. 2 The digital elevation model (DEM) constructed by ANUDEM interpolation at different spatial resolutions. Red and green colors indicate high and low altitude, respectively

Table 2 List of flow direction algorithms used in this study (Wilson 2018)

Flow direction algorithm	Description	References
BR: Braunschweiger relief model	The direction of flow is maximum limited to three neighboring cells, to avoid excessive flow's dispersion	Bauer et al. (1985)
D8: deterministic eight-node algorithm	Permits flow to one of eight neighbors based on the direction of steepest descent	O'Callaghan and Mark (1984)
DI: deterministic infinite-node algorithm	Specifies the flow direction continuously and assigns flow direction to one or at most two downslope cells	Tarboton (1997)
MFD: multiple flow direction	Permits flow to multiple downslope neighbors using slope-weighted methods	Freeman (1991) and Quinn et al. (1991)
MGD: multiple flow direction based on maximum downslope gradient	Permits flow to multiple downslope neighbors using slope weighted methods that vary as a linear function of maximum downslope gradient	Qin et al. (2011)
Rho 8: randomized eight-node algorithm	Stochastic version of D8 that directs flow to one of eight neighbors and produces a mean flow direction equal to aspect	Fairfield and Leymarie (1991)
TFD: triangular multiple flow direction algorithm	Divides each cell into eight triangular facets, calculates local slope directions and gradients around each cell, and distributes flow in downslope directions using a slope-weighted	Seibert and McGlynn (2007)

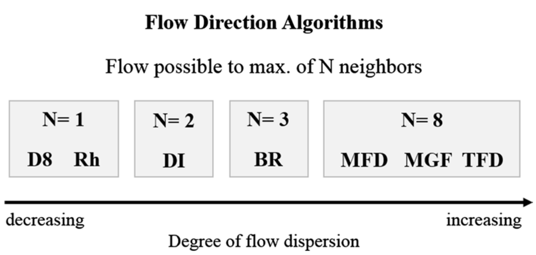

was used to illustrate the trend of changes in terrain attribute statistics. A flowchart of this study is shown in Fig. 3.

Results and discussion

The statistical analysis of elevation and slope gradient in five spatial resolutions are presented (Table 3). The mean of elevation attribute is not changed significantly with decreasing spatial resolution, but at a meticulous look the mean values are associated with an increase. This is consistent with the findings of Han et al. (2018) and Khanifar et al. (2019). The importance of elevation attribute in soil erosion is due to its influence on climate characteristics, soil weathering rate and vegetation cover distribution. Khanifar et al. (2019) stated that the elevation was negatively correlated with soil aggregate stability, which is an indicator of soil erodibility. Figure 2 shows a portion of the study area in five spatial resolutions. As Fig. 2 presents, the distribution of elevation values did not alter with decreasing spatial resolution. Other descriptive statistics of the elevation attribute have low rate of changes, which based on the observations can be stated that this rate of alterations is visible in interpolation to bigger pixel size. It can be seen from Table 3 that by decreasing the DEM spatial resolution the mean and standard deviation values of slope gradient slightly decrease. The most effect of upscaling on the slope gradient was related to the maximum statistic so that a 34 degree difference between spatial resolutions of 0.25 m and 3 m was observed. However, minimum values remain constant at all spatial resolutions. As the pixel dimension increases when constructing a DEM (upscaling), the potential information of some details of short, steep slopes and microscale topographic ruggedness is diluted in large pixels, which causes the land surface to be somewhat flat (smoothing effect) and the slope values alter. The slope gradient is a factor affecting the velocity of surface and subsurface flow of water. By decreasing in interpolated grid pixel size, the estimation of slope and soil erosion will enhance (Kienzle 2004). The mean and standard deviation values of the catchment area (upslope area) attributes (flow accumulation multiplied by pixel area) obtained based on different flow direction algorithms in the five given scales are presented (Figs. 4, 5). As the DEM spatial resolution declines, the mean value of catchment area increases (Fig. 4), because the calculation of the catchment area is based on the area of the pixel in which

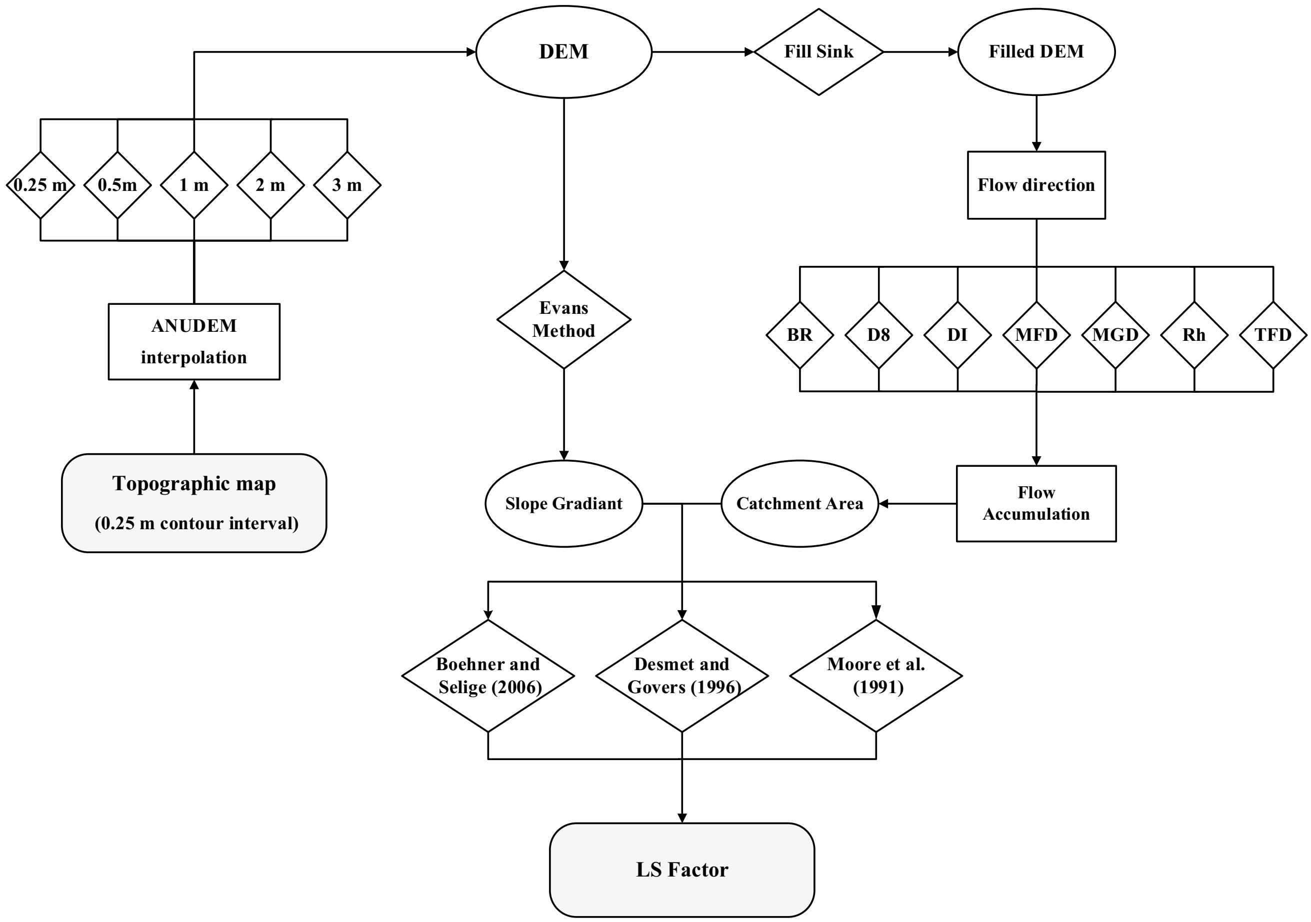

Fig. 3 The flowchart of different parts of study design

Table 3 Statistical summary of two terrain attributes for 5 DEM cell sizes

Scale	Min	Max	Mean	SD
DEM				
0.25	65.785	96.236	79.161	5.503
0.5	65.956	96.238	79.161	5.500
1	65.555	96.192	79.163	5.502
2	65.962	96.041	79.162	5.493
3	66.003	96.055	79.167	5.478
Slope gradient				
0.25	0.000	1.331	0.071	0.112
0.5	0.000	1.055	0.069	0.109
1	0.000	0.904	0.067	0.105
2	0.000	0.770	0.064	0.096
3	0.000	0.727	0.062	0.09

the flows were drained. By decreasing the spatial resolution, the pixel coverage area becomes larger and more flow from the upslope area is accumulated. The effectiveness of the DEM scale on the catchment area at different landscape positions is quite different; therefore this effect decreases from upstream to downstream (Wu et al. 2008; Yang et al. 2011). The highest and lowest mean values of catchment area in all scales were obtained by MFD and BR algorithms, respectively (e.g., the mean value of catchment area at 1 m scale; MFD algorithm: 143.13 and BR algorithm: 77.90 m^2). This is consistent with the findings of Wilson et al. (2007) that the specific catchment area obtained based on the MFD algorithm has the highest mean value among all investigated flow direction algorithms (D8, Rh, DEMON and DI). By decreasing DEM spatial resolution, the standard deviation value of the catchment area increases; at all scales the highest and lowest standard deviations calculated belong to the catchment area attributes obtained using Rh and BR algorithms, respectively. Statistics of the BR algorithm show that by decreasing spatial resolution, the hydrological behavior difference between this algorithm and other flow direction algorithms was increased. This observation can confirm that at high spatial resolutions, different flow direction algorithms have close final performance (in catchment area obtaining) despite the difference in flow distribution to neighboring cells. This is contrasted with the findings

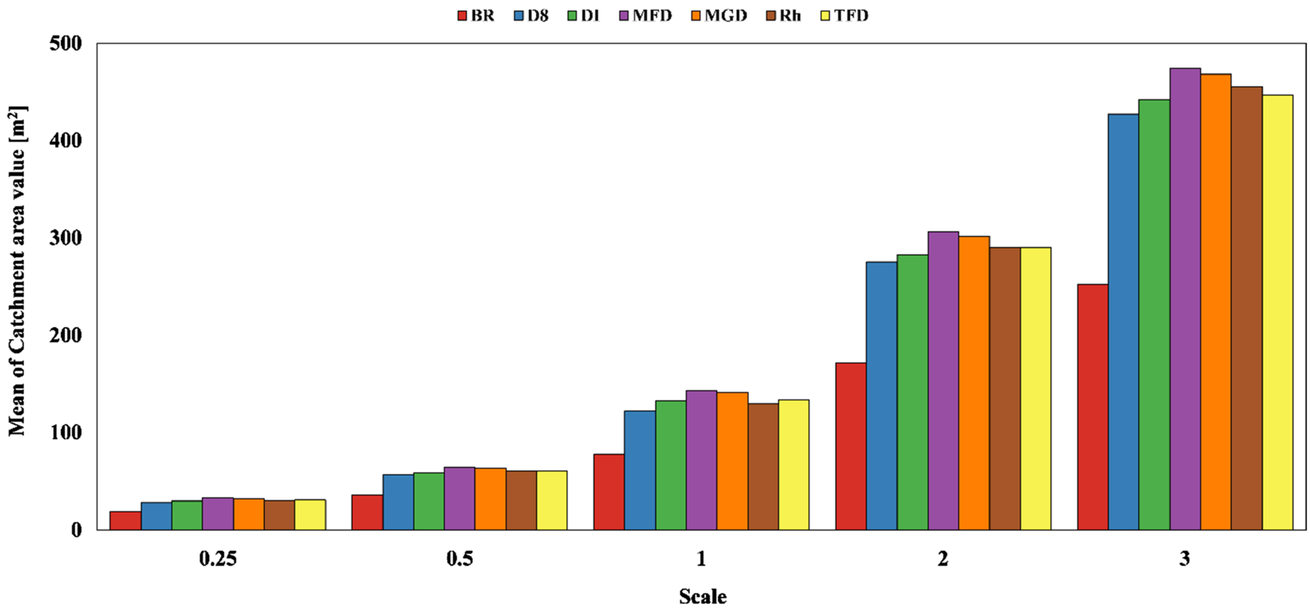

Fig. 4 Mean values of catchment area attributes obtained based on different flow direction algorithms at five scales

Fig. 5 Standard deviation values of catchment area attributes obtained based on different flow direction algorithms at five scales

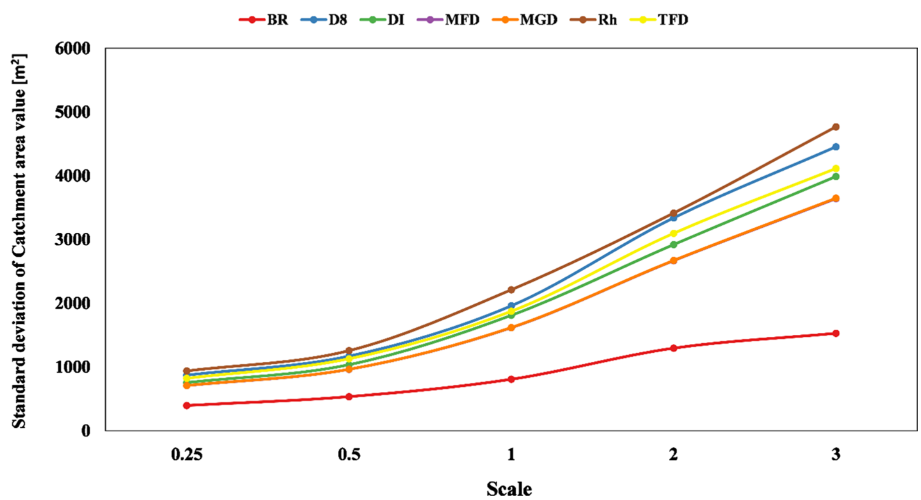

of Park et al. (2009) that by increasing the scale, difference between the mean values of catchment area obtained based on different flow direction algorithms under investigation would be smaller. The least difference between the mean values at all scales is between the catchment area attributes obtained by the two algorithms TFD and Rh. For all spatial resolutions, the standard deviation of the MFD and MGD catchment area overlaps. In this research, only two single flow direction algorithms of Rh and D8 were used for modeling the catchment area. These two algorithms have the highest value of standard deviation among all types of flow direction algorithms. Wilson et al. (2000) observed that the Rh algorithm produces lower catchment area than the D8 method, which is due to breaking of linear flow paths and improving flow concentration at convergence segments of the hillslope (Park et al. 2009). However, the Rh-based catchment area had higher mean values than D8 at all scales (see further in the next section).

The mean and standard deviation statistics of the LS factors calculated by three different methods based on different flow direction algorithms at five spatial resolutions (0.25–3 m) are presented in Figs. 6 and 7, respectively. By upscaling, the changing trend of the LS factor statistics values in two methods of Boehner and Selige (2006) and Moore et al. (1991) is similar in all flow direction algorithms, but shows an inverse relationship with Desmet and Govers (1996) method. The changes in these statistics are due to the catchment area (CA in factor L) (corresponds

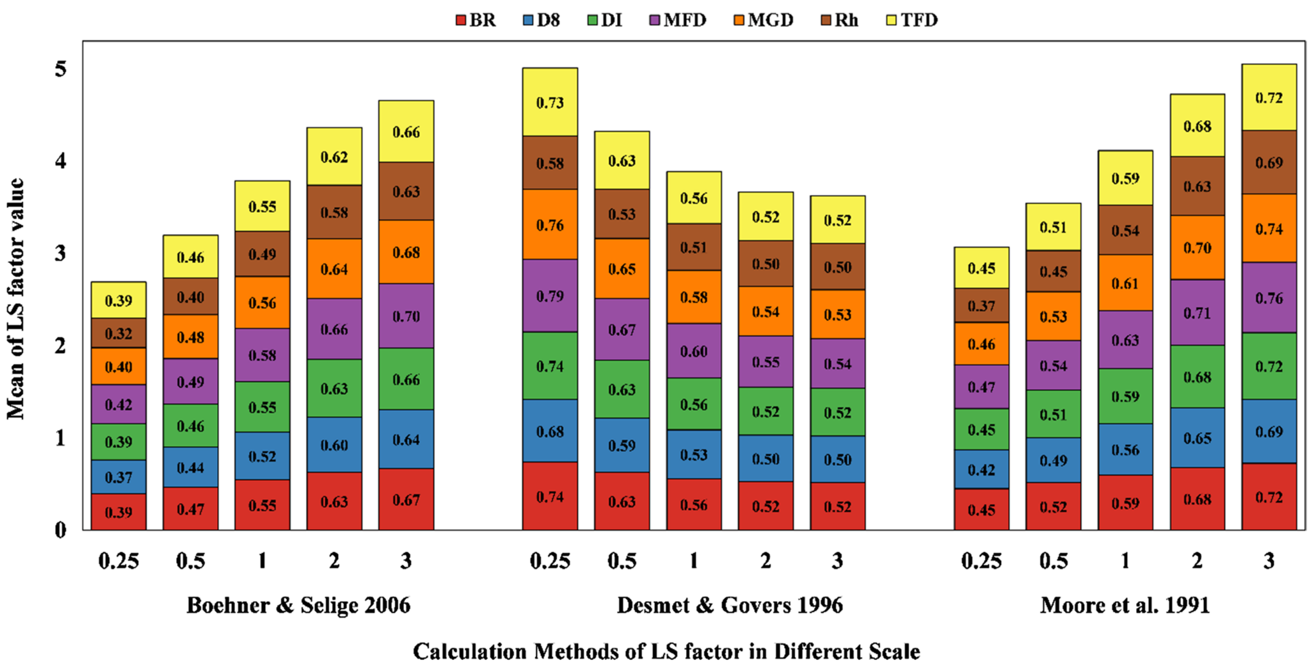

Fig. 6 The mean values of the LS factors calculated by three different methods based on different flow direction algorithms at five scales (0.25–3 m)

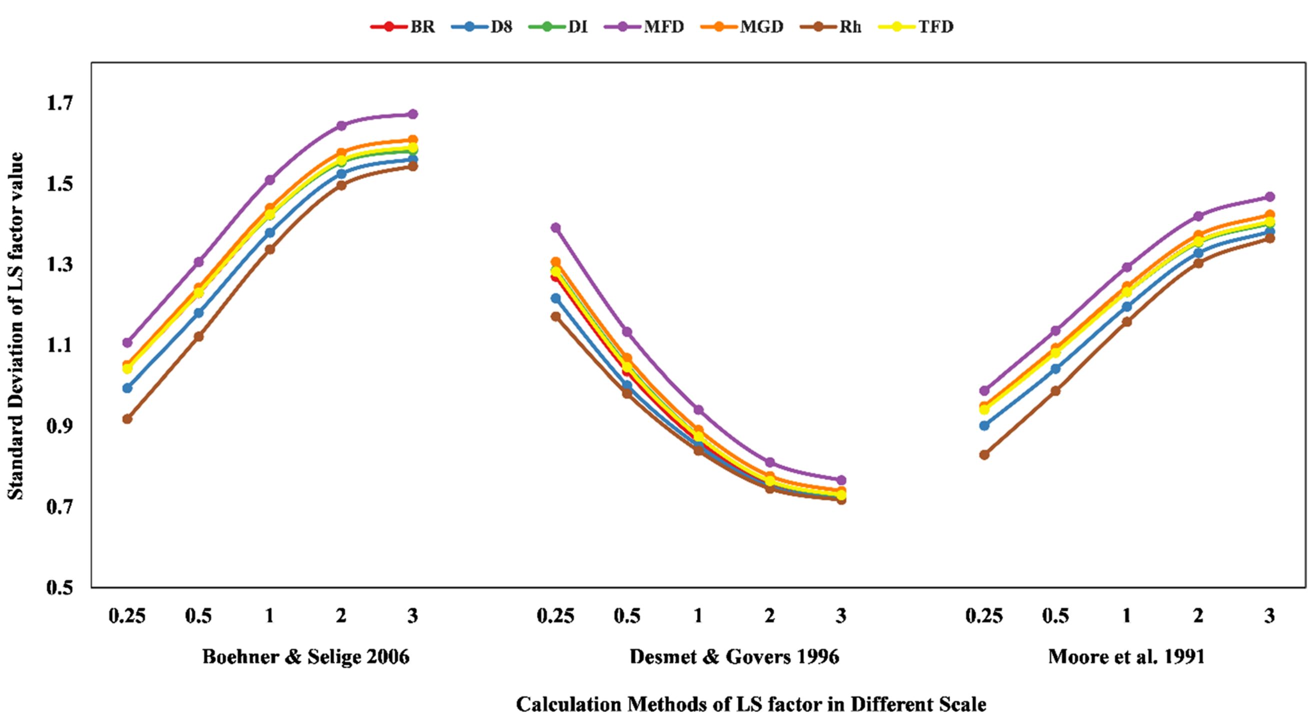

Fig. 7 The standard deviation values of the LS factors calculated by three different methods based on different flow direction algorithms at five scales (0.25–3 m)

to Han et al. 2018) because as spatial resolution decreases, the slope gradient decreases. Therefore, by decreasing the DEM spatial resolution, the mean and standard deviation values of the LS factor in both Boehner and Selige (2006) and Moore et al. (1991) methods increase and in the Desmet and Govers (1996) method decrease. The slope gradient is the most important factor in controlling the LS factor value, such that an adjusted coefficient of determination (R^2_adj) greater than 0.9 was observed between the slope gradient and the LS factor. (Due to space constraints, the results were not mentioned here, but Khanifar et al. 2019 point to this.) Therefore, according to the LS factor change rate against the scale (Fig. 6), it seems that the effect of slope length in these methods compared to the slope factor is not well considered. Application of these three methods to estimate LS factor showed a meaningful error; accordingly, these methods are not appropriate to estimate topographical indices in the watersheds (Azizian and Kohi 2019). In similar spatial resolution and flow direction algorithm, the mean value of the LS factor calculated by Moore et al. (1991) is higher than Boehner and Selige (2006) method. Hrabalikova and Janeček (2017) found that the mean value of two L and S factors calculated by Moore et al. (1991) method is higher than Desmet and Govers (1996) method. Desmet and Govers (1996) method found a very low difference between the mean values of LS factors at 2 and 3 m scales. The LS factors used the MFD flow direction algorithm to obtain the catchment area have the highest mean and standard deviation values at all scales. The mean of the catchment area attributes obtained by this flow direction algorithm is higher than other algorithms (Fig. 4). The BR flow direction algorithm that produced a completely different catchment area compared to other algorithms (especially at large scales) has little statistical difference in computing LS factors by these three methods with the two MGD and DI algorithms at all scales. The lowest mean and standard deviation values of LS factors at all spatial resolutions were obtained based on two single flow direction algorithms of Rh and D8. The statistical difference between the LS factors calculated based on Rh and D8 algorithms by these three methods decreases with declining spatial resolution, especially after 2 m.

The map of the calculated LS factors based on two single flow direction algorithms of Rh and D8 and the multiple flow direction algorithm of TFD are shown in Figs. 8, 9 and 10, respectively. The map of the LS factors presented in Figs. 8 and 9 shows the streaking effect, which is due to the use of the single flow direction algorithms in producing the catchment area attribute used in the LS factor computational equations. This effect is more intense in calculations based on the Rh algorithm and was occurred at all scales. The weakness of this kind of flow direction algorithms for handling divergent flows in areas with complex topography and convex hillslopes causes this effect. However, these types of flow direction algorithms, and in particular D8, are useful in extracting channel networks and watershed boundaries and are used in many GIS software packages (Gruber and Peckham 2009). According to Fig. 10, the streaking effect has been reduced by using a multiple flow direction algorithm because of the ability of this type of algorithm to handle the effects of diverging flows in modeling. Multiple flow direction algorithms are powerful in handling sub-grid affects; for example, a horizontal ridge pixel will drain the flow towards the opposite sides (Gruber and Peckham 2009).

To investigate the frequency distribution of LS factors calculated by three different methods based on seven types of flow direction algorithms at 0.25 and 3 m scales, their values in five categories (0–0.1, 0.1–0.2, 0.2–0.5, 0.5–2 and > 2) were grouped and the results were plotted

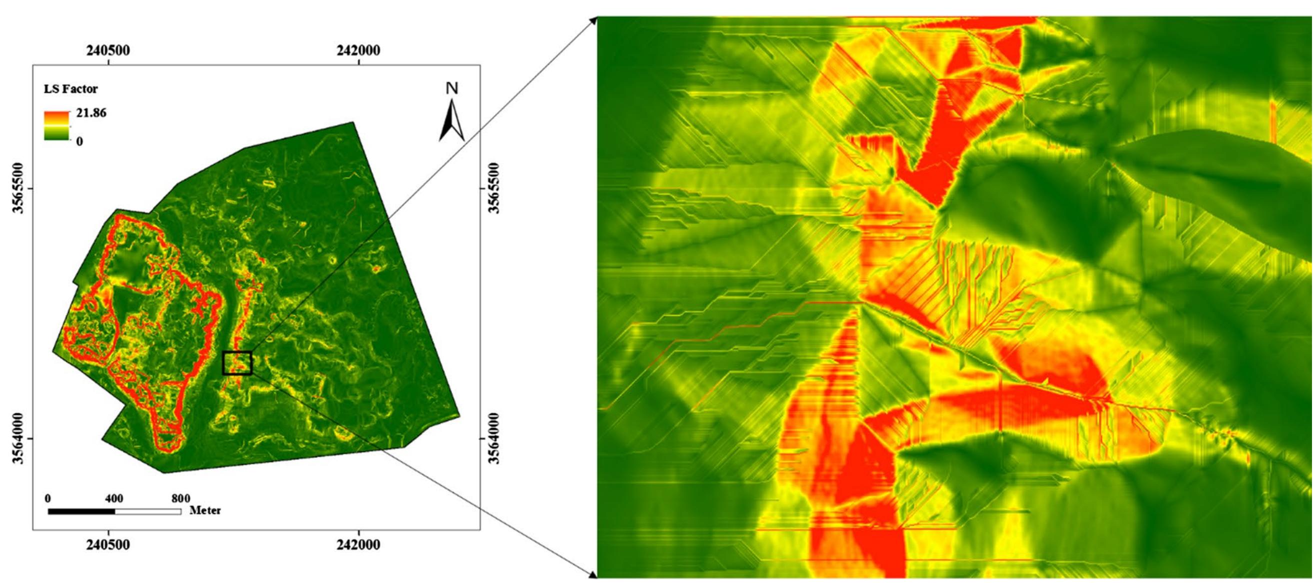

Fig. 8 LS factor map calculated by the Moore et al. (1991) method fitted algorithm based on D8 algorithm at 0.25 m scale

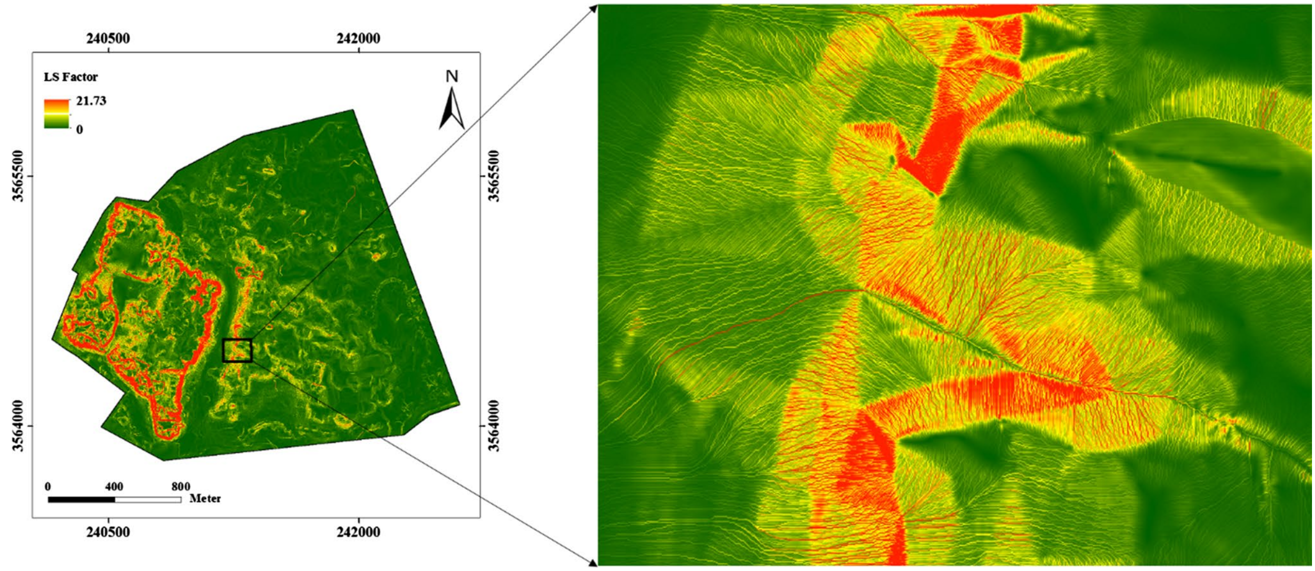

Fig. 9 LS factor map calculated by the Moore et al. (1991) method fitted algorithm based on Rh algorithm at 0.25 m scale

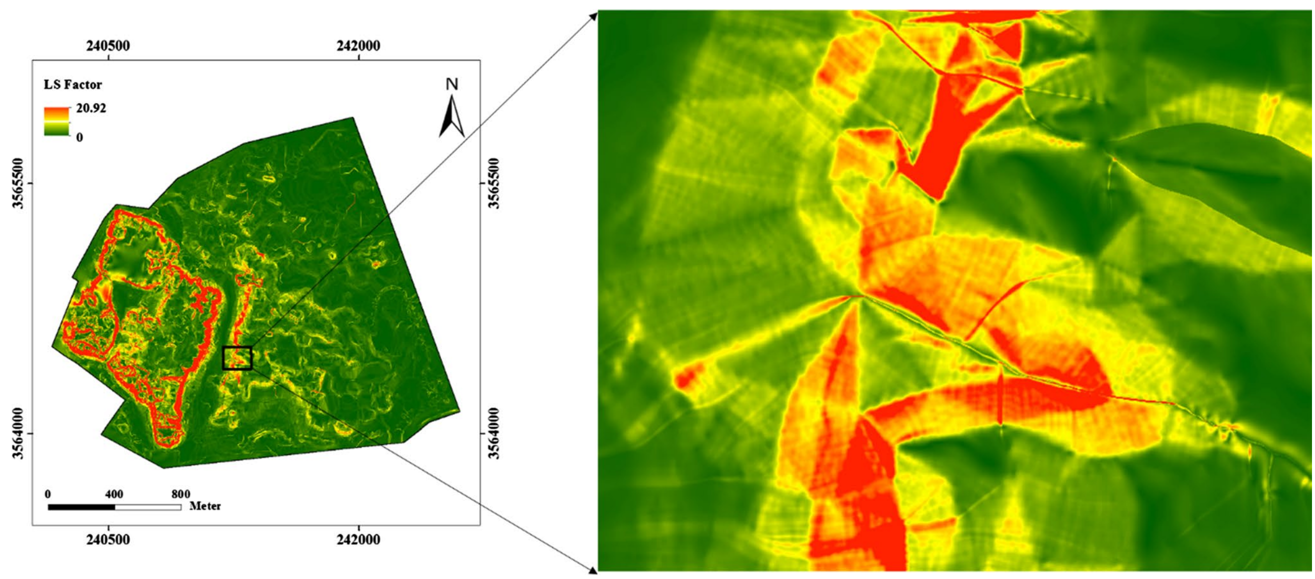

Fig. 10 LS factor map calculated by the Moore et al. (1991) method fitted algorithm based on TFD algorithm at 0.25 m scale

(Figs. 11, 12). At 0.25 m spatial resolution, the highest distribution of the LS factors calculated by Boehner and Selige (2006) and Moore et al. (1991) methods is in first group (0–0.1) with frequencies ranging from 42 to 62% for a variety of flow direction algorithms, but in the Desmet and Govers (1996) method the highest distribution of LS factors values is in the third group (0.2–0.5) with a frequency of about 35%. Frequency distribution of LS factors calculated based on two Rh and D8 algorithms in each of these three methods has a difference with other flow direction algorithms at 0.25 m scale, in which this difference decreases with increasing scale. At a spatial resolution of 3 m, the highest frequency of LS factor values calculated by Moore et al. (1991), Boehner and Selige (2006) and Desmet and Govers (1996) methods is distributed in the first (0–0.1), second (0.1–0.2) and third groups (0.2–0.5), respectively. Frequency distribution differences between the Boehner and Selige (2006) and Moore et al. (1991) methods are lower at the 0.25 scale, but at the 3-m scale, the distribution of these two methods has a higher difference. In the three methods of calculating the LS factor, the lowest frequency distribution is related to the fifth

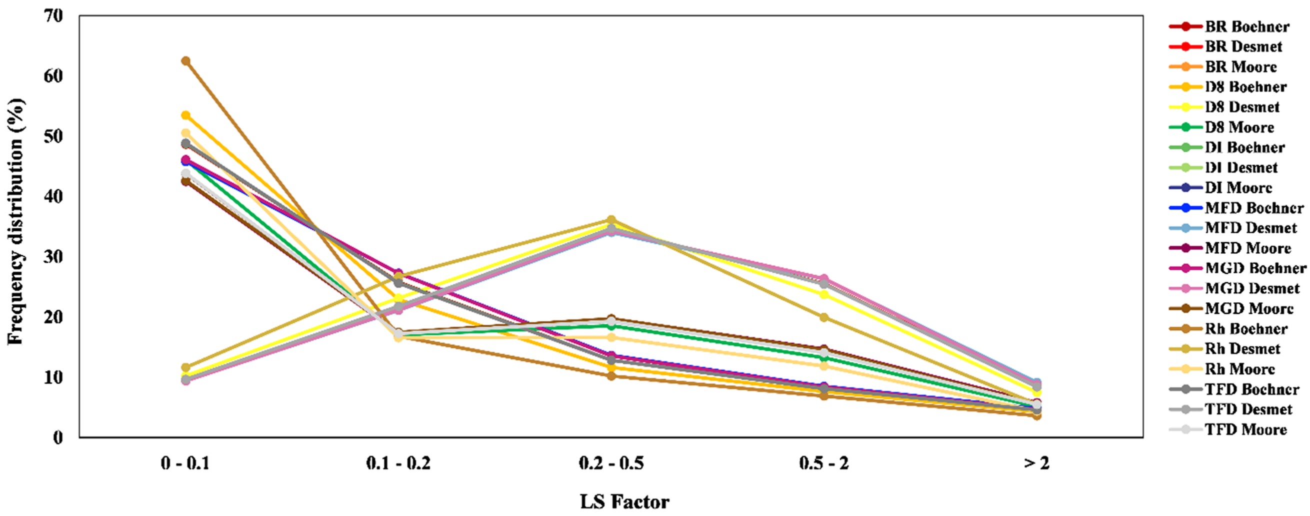

Fig. 11 Frequency distribution of LS factor values calculated by three different methods based on seven flow direction algorithms at 0.25 m scale

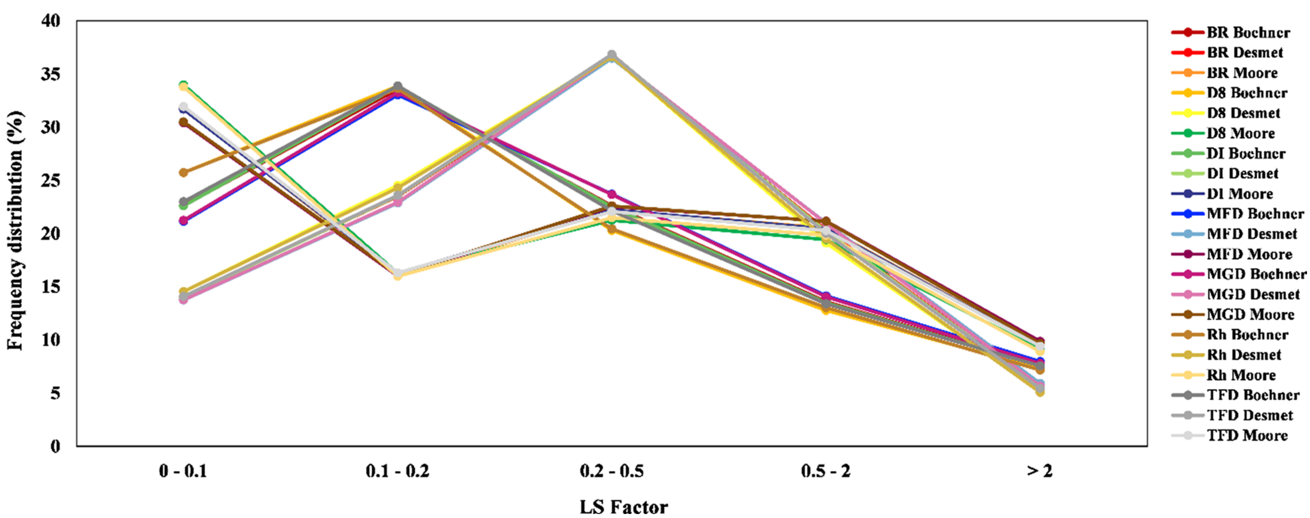

Fig. 12 Frequency distribution of LS factor values calculated by three different methods based on seven flow direction algorithms at 3 m scale

category (> 2), in which the Desmet and Govers (1996) and Moore et al. (1991) methods have more frequency in this category at the 0.25- and 2-m scales, respectively.

Conclusion

The results of this study reveal that by using the coarser spatial resolution the slope gradient decreases, which can be due to the effect of topographic smoothing. By decreasing the spatial resolution, the mean and standard deviation of all catchment area attributes produced based on the seven types of flow direction algorithms increased. The catchment area produced based on the MFD algorithm has the highest mean value compared to other algorithms. At high spatial resolutions, the different flow direction algorithms despite the difference in the flow distribution to the neighboring cells result in the production of catchment area attributes with a bit difference. By decreasing the DEM spatial resolution, the LS factor values calculated in Boehner and Selige (2006) and Moore et al. (1991) methods increase whereas in Desmet and Govers (1996) method decline. The single flow direction algorithms of Rh and D8 help to calculate the lowest mean values of LS factors at all spatial resolutions and in the LS factors map calculated based on these two algorithms can be seen the streak effect due to their weakness in handling divergent flows but this effect was solved by applying multiple flow direction algorithms. The difference between the frequency distribution of the LS factors calculated by these three methods increases with decreasing spatial resolution. An overview of the results of this study indicates the importance of scale and selection of the type of method for calculating the LS factor, which is much higher than the type of flow direction algorithm used to obtain the catchment area.

Acknowledgements The authors of this article would like to thank Mr. Heidarizadeh and Mr. Ahmadzadeh for their cooperation in providing the topographic map of the Susa ancient site.

References

Azizian A, Kohi S (2019) Evaluating the effect of different methods for calculating topographic factor on sediment delivery rate based on RUSLE model (Case study: Barajin catchment, Qazvin). Iran Water Resour Res 14(5):304–317 **(Persian literature)**

Bauer J, Rohdenburg H, Bork H-R (1985) Ein Digitales Reliefmodell als Vorraussetzung fuer ein deterministisches Modell der Wasser- und Stoff-Fluesse. Landschaftsgenese und Landschaftsoekologie, H.10, 1–15

Boehner J, Selige T (2006) Spatial prediction of soil attributes using terrain analysis and climate regionalisation. In: Boehner J, McCloy KR, Strobl J (eds) SAGA—analysis and modelling applications. Goettinger Geographische Abhandlungen, vol 115, pp 13–27

Deng Y, Wilson JP, Bauer BO (2007) DEM resolution dependencies of terrain attributes across a landscape. Int J Geogr Inf Sci 21(2):187–213

Desmet PJJ, Govers G (1996) A GIS procedure for automatically calculating the USLE LS factor on topographically complex landscape units. J Soil Water Conserv 51(5):427–433

Evans IS (1979) An integrated system of terrain analysis and slope mapping. Final report on grant DA-ERO-591-73-G0040, University of Durham, England

Florinsky I (2016) Digital terrain analysis in soil science and geology, 2nd edn. Academic Press, Amsterdam, pp 265–270

Freeman TG (1991) Calculating catchment area with divergent flow based on a regular grid. Comput Geosci 17(3):413–422

Fairfield J, Leymarie P (1991) Drainage networks from grid digital elevation models. Water Resour Res 27:709–717

Gessler PE (1996) Statistical soil–landscape modelling for environmental management. PhD thesis, Australian National University

Gruber S, Peckham S (2009) Land-surface parameters and objects in hydrology. In: Hengle T, Reuter HI (eds) Geomorphometry: concepts, software, applications. Elsevier, Amsterdam, pp 171–194

Han X, Liu J, Mitra S, Li X, Srivastava P, Guzman SM, Chen X (2018) Selection of optimal scales for soil depth prediction on headwater hillslopes: a modeling approach. CATENA 163:257–275

Howland MD, Jones IW, Najjar M, Levy TE (2018) Quantifying the effects of erosion on archaeological sites with low-altitude aerial photography, structure from motion, and GIS: a case study from southern Jordan. J Archaeol Sci 90:62–70

Hrabalikova M, Janeček M (2017) Comparison of different approaches to LS factor calculations based on a measured soil loss under simulated rainfall. Soil Water Res 12(2):69–77

Iranian Cultural Heritage, Handicrafts and Tourism Organization (ICHHTO) (2015) Report of evaluation of the nomination of the “Susa” for inscription on the World Heritage List

Khanifar J, Khademalrasoul A, Amerikhah H (2019) Effects of digital elevation model (DEM) spatial resolution on soil landscape analysis (case study Raakat watershed of Izeh, Khuzestan Province). Appl Soil Res (accepted paper) **(Persian literature)**

Kienzle S (2004) The effect of DEM raster resolution on first order, second order and compound terrain derivatives. Trans GIS 8(1):83–111

Kinner DA (2003) Multi-scale estimation of erosion and deposition in the Mississippi river basin. PhD thesis, University of Colorado

Li Z, Zhu Q, Gold C (2005) Digital terrain modeling: principles and methodology. CRC Press, Boca Raton, pp 267–284

McKenzie NJ, Ryan PJ (1999) Spatial prediction of soil properties using environmental correlation. Geoderma 89(1):67–94

McCool DK, Foster GR, Mutchler CK, Meyer LD (1989) Revised slope length factor in the universal soil loss equation. Trans Am Soc Agr Eng 32:1571–1576

Moore ID, Grayson RB, Ladson AR (1991) Digital terrain modelling: a review of hydrological, geomorphological, and biological applications. Hydrol Process 5(1):3–30

O’Callaghan JF, Mark DM (1984) The extraction of drainage networks from digital elevation data. Comput Vis Graph Image Process 28(3):323–344

Park SJ, Rüecker GR, Agyare WA, Akramhanov A, Kim D, Velk PLG (2009) Influence of grid cell size and flow routing algorithm on soil–landform modeling. J Korean Geogr Soc 44(2):122–145

Pike RJ, Evans IS, Hengl T (2009) Geomorphometry: a brief guide. In: Hengle T, Reuter HI (eds) Geomorphometry: concepts, software, applications. Elsevier, Amsterdam, pp 3–30

Qin CZ, Zhu AX, Pei T, Li BL, Scholten T, Behrens T, Zhou CH (2011) An approach to computing topographic wetness index based on maximum downslope gradient. Precis Agric 12(1):32–43

Quinn PFBJ, Beven K, Chevallier P, Planchon O (1991) The prediction of hillslope flow paths for distributed hydrological modelling using digital terrain models. Hydrol Process 5(1):59–79

Renard KG, Foster GR, Weesies GA, Porter JP (1991) Revised universal soil loss equation. J Soil Water Conserv 46(1):30–33

Seibert J, McGlynn BL (2007) A new triangular multiple flow direction algorithm for computing upslope areas from gridded digital elevation models. Water Resour Res 43(4):1–8

Tarboton DG (1997) A new method for the determination of flow directions and upslope areas in grid digital elevation models. Water Resour Res 33(2):309–319

Wilson, J. P. (2018). Environmental Applications of Digital Terrain Modeling. John Wiley & Sons.

Wilson JP, Repetto PL, Snyder RD (2000) Effect of data source, grid resolution, and flow routing method on computed topographic attribute. In: Wilson JP, Gallant JC (eds) Terrain analysis: principles and application. Wiley, New York, pp 133–161

Wilson JP, Lam CS, Deng Y (2007) Comparison of the performance of flow-routing algorithms used in GIS-based hydrologic analysis. Hydrol Process Int J 21(8):1026–1044

Wu S, Li J, Huang GH (2008) A study on DEM-derived primary topographic attributes for hydrologic applications: sensitivity to elevation data resolution. Appl Geogr 28(3):210–223

Yang X, Tang G, Xiao C, Gao Y, Zhu S (2011) The scaling method of specific catchment area from DEMs. J Geog Sci 21(4):689–704

Zhang W, Montgomery DR (1994) Digital elevation model grid size, landscape representation, and hydrologic simulations. Water Resour Res 30(4):1019–1028

Zhang HY, Shi ZH, Fang NF, Guo MH (2015) Linking watershed geomorphic characteristics to sediment yield: evidence from the Loess Plateau of China. Geomorphology 234:19–27

Zhou Q, Liu X (2002) Error assessment of grid-based flow routing algorithms used in hydrological models. Int J Geogr Inf Sci 16(8):819–842

Zhu X (2016) GIS for environmental applications: a practical approach. Routledge, London